JACS
JOURNAL OF THE AMERICAN CHEMICAL SOCIETY
pubs.acs.org/JACS
Article

Ancillary Ligand Steric Effects and Cyclometalating Ligand Substituents Control Excited-State Decay Kinetics in Red-Phosphorescent Platinum Complexes

Sungwon Yoon and Thomas S. Teets*

Cite This: J. Am. Chem. Soc. 2024, 146, 28407−28413
Read Online

ABSTRACT: Achieving high-efficiency red phosphorescence remains a significant challenge, especially in cyclometalated platinum complexes where radiative rates are inherently slower than their iridium counterparts. In this work, six red-emitting cyclometalated platinum complexes of the formula Pt(C^N)[(Ar)-acNac] (C^N is the cyclometalating ligand, and (Ar)acNac is an aryl-substituted β-ketoiminate ancillary ligand) were synthesized and characterized. Two C^N ligands were employed, 1-phenyl-isoquinoline (piq) and its cyano-substituted analogue 1-phenyl-isoquinoline-4-carbonitrile (piqCN), which both result in red phosphorescence in cyclometalated platinum complexes. These were paired with three (Ar)acNac ligands that are sterically differentiated via the *N*-aryl group, which is phenyl in the unsubstituted analogue (Ph)acNac and 2,6-dimethylphenyl or 2,6-diisopropylphenyl in the sterically encumbered analogues. An in-depth photophysical analysis of all compounds was performed and compared to the related compounds with the acetylacetonate (acac) ancillary ligand. While quantum yields are modest in the unsubstituted (Ph)acNac complexes, steric bulk on the β-ketoiminate has a pronounced effect on the excited-state dynamics and can lead to photoluminescence quantum yields of more than 0.50 in both solution and transparent polymer films, with the photoluminescence $\lambda_{max} \sim 630$ nm. We show that both steric effects on the electron-rich β-ketoiminate ancillary ligands and the cyano substituent on the cyclometalating ligand play a role in achieving high-efficiency phosphorescence in the red region.

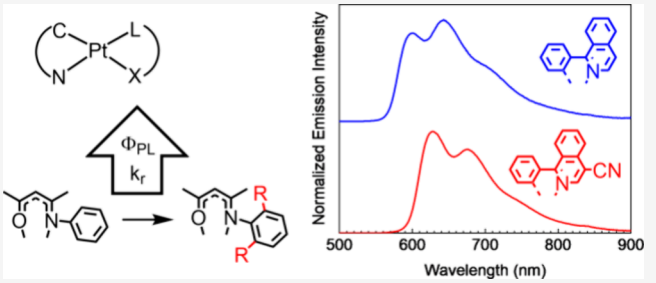

INTRODUCTION

Phosphorescent platinum(II) compounds have gained attention owing to their various applications such as optoelectronics,[1] solar cells,[2] photocatalysis,[3−5] sensing,[6,7] and stimuli-responsive materials.[8] A platinum porphyrin compound was the first phosphorescent dopant used in an organic light-emitting diode (OLED),[9] as the premier demonstration that phosphorescent transition-metal compounds can increase OLED efficiency by harvesting both singlet and triplet excitons, enabled by efficient intersystem crossing (ISC). Although the most successful OLED phosphors are based on Ir(III),[10−12] complexes of Pt(II)[13−16] remain prominent in OLED applications. Many platinum-based phosphors, particularly those with long-wavelength phosphorescence in the red region, luminesce from aggregated states which require high concentrations.[17] Consequently, extensive research has been dedicated to diplatinum complexes to achieve long-wavelength phosphorescence without aggregation.[18−22] There are also some notable examples of mononuclear platinum complexes with red to deep-red phosphorescence, many featuring terdentate or tetradentate chelating ligands.[23−30] Although impressive outcomes have been made, there is a demand for further development of novel luminescent materials, and we propose that heteroleptic bis-bidentate complexes may offer simpler syntheses and greater modularity, so strategies that can augment their performance to be on par with the terdentate and tetradentate analogues would be desirable.

Red-emitting phosphors have the intrinsic challenge of relatively low quantum yields. Due to the energy gap law,[31,32] the nonradiative decay constant (k_{nr}) demonstrates an inverse relationship with the energy difference between the ground and excited states. In addition, according to second-order perturbation theory, the rate of radiative rate constant (k_r) exhibits a cubic dependence on the energy gap.[33] These lead to a decrease in k_r and an increase in k_{nr} for lower-energy emitters, which contribute to the low quantum yields. Low radiative rate constants are a particularly significant challenge in phosphorescent platinum complexes, given the dependence of k_r on the spin−orbit interactions between the ^{3}MLCT states and higher-

Received: July 24, 2024
Revised: September 22, 2024
Accepted: September 26, 2024
Published: October 2, 2024

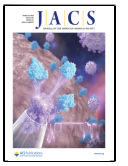

https://doi.org/10.1021/jacs.4c10110
J. Am. Chem. Soc. 2024, 146, 28407−28413

lying ^{1}MLCT states, with quantum mechanics dictating that the interacting states involve different 5*d* orbital parentage.[33,34] In octahedral Ir(III) complexes, the three filled 5*dπ* orbitals are energetically proximate, which results in closely spaced MLCT states, facilitating efficient mixing of these states and leads to stronger spin−orbit coupling (SOC).[35] On the other hand, square planar 5d^8 platinum complexes have a larger splitting between the highest occupied 5*d* orbital and the lower-lying 5d*π* orbitals, resulting in a larger gap between MLCT states that leads to weaker SOC.

We have succeeded in augmenting k_r values in red-phosphorescent bis-cyclometalated iridium complexes, Ir(C^N)$_2$(L^X), using nitrogen-donor, electron-rich ancillary ligands (L^X).[36,37] Our results are consistent with idea that these electron-rich ancillary ligands increase ^{3}MLCT character and SOC in the luminescent excited state, increasing k_r. Using this approach, we achieved photoluminescence quantum yields (Φ_{PL}) as high as 0.80. We hypothesized that similar effects can be beneficial in red-phosphorescent cyclometalated platinum complexes, but anticipated additional challenges and distinct structure−property relationships would emerge, owing to the different coordination geometry, disparate spin−orbit coupling pathways, and increased propensity for aggregation in Pt(II) complexes relative to Ir(III) (see above).

In this work, we demonstrate that cyclometalated platinum complexes with substituted *β*-ketoiminate ((Ar)acNac) ancillary ligands can achieve high phosphorescence quantum yields in the red region. In iridium(III) complexes, limited steric perturbations of the ancillary ligand are possible owing to the crowded octahedral coordination environment, and the effects of steric augmentation are generally modest.[38,39] In contrast, in the square planar platinum complexes introduced here, the steric profile of the (Ar)acNac ligand can be tuned in a significant way, giving the new insight that steric effects play a major role in controlling the excited-state decay kinetics and optimizing the quantum yields. Six new platinum complexes are described using three different (Ar)acNac ligands paired with two cyclometalating ligands (C^N) that were chosen to target red phosphorescence.[40,41] A comprehensive photophysical analysis in toluene solution and in transparent polymer film provides insights into the impacts on excited-state dynamics and phosphorescence quantum yields. Very good quantum yields in excess of 0.5 can be achieved in both solution and film, and there is evidence that the ancillary ligand steric profile also plays a role in limiting aggregation in film samples.

RESULTS AND DISCUSSION

Synthesis and Structural Characterization. The general synthetic procedure for the six new Pt(C^N)[(Ar)acNac] complexes is shown in Scheme 1, where C^N is the cyclometalating ligand 1-phenylisoquinoline (piq) or 1-phenylisoquinoline-4-carbonitrile (piqCN), and (Ar)acNac is a substituted *β*-ketoiminate ligand. Scheme 1 also shows the structures of Pt(C^N)(acac) complexes (acac = acetylacetonate) used as a point of comparison and synthesized as described in the literature for related compounds.[13] The cyclometalating ligands were chosen to target emission in the red region of the spectrum, and the (Ar)acNac class is appealing for this study since it is one of the most successful ancillary ligand classes in supporting high-efficiency red phosphorescence in cyclometalated iridium complexes.[36,38,39] Distinct from our previous work on this ancillary ligand class, the steric profile of the (Ar)acNac ligand is progressively augmented via the *N*-aryl group, which is phenyl in the parent (Ph)acNac ligand, 2,6-dimethylphenyl in (dmp)acNac, and 2,6-diisopropylphenyl in (dipp)acNac. The platinum complexes were synthesized by treating [Pt(C^N)(*μ*-Cl)]$_2$ with the potassium salt of the corresponding (Ar)acNac ligand in toluene at 100 °C.[42] The complexes were accessed in isolated yields of 24−41% and were characterized by ^{1}H and ^{13}C{^{1}H} NMR spectroscopy (Figures S12−S23), and high-resolution mass spectrometry. Scheme 1 also shows the numbering scheme used to abbreviate the complexes, where each is given a unique number (**1**−**6**) with the appended superscripts indicating the substituents on the cyclometalating ligand (H for piq, CN for piqCN) and the identity of the *N*-aryl ring (Ph, dmp, or dipp).

Scheme 1. Synthetic Procedure for the Pt(II) Complexes

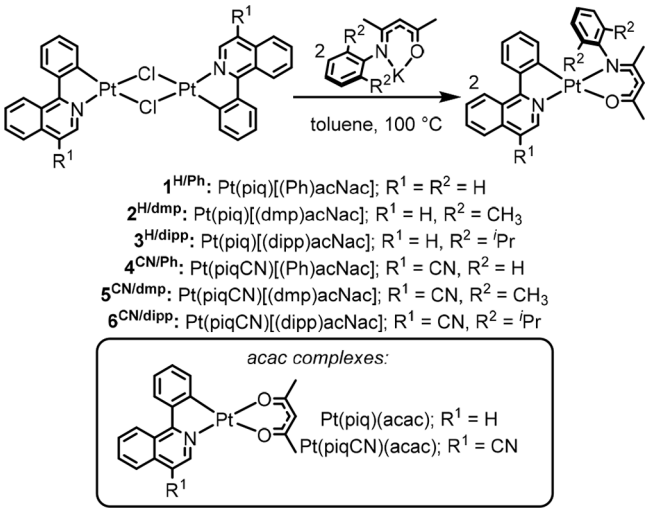

Single crystals of complexes **1**$^{H/Ph}$, **2**$^{H/dmp}$, and **6**$^{CN/dipp}$ were characterized by X-ray diffraction. Their molecular structures are shown in Figure 1 with refinement data summarized in Table S1. An approximately square planar geometry about the platinum(II) center is observed, and a *trans* disposition of the

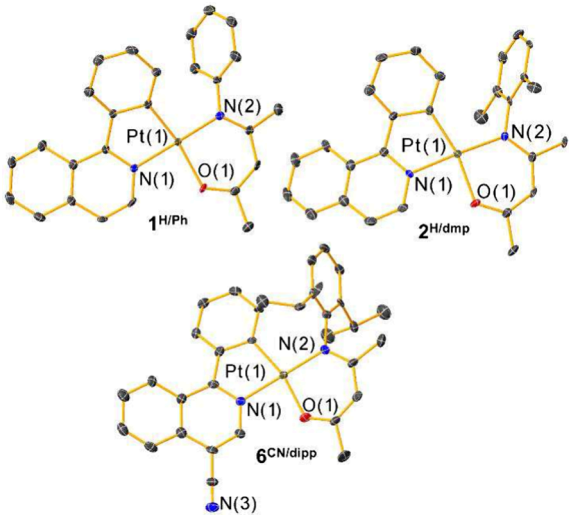

Figure 1. Molecular structures of complexes **1**$^{H/Ph}$, **2**$^{H/dmp}$, and **6**$^{CN/dipp}$, determined by single-crystal X-ray diffraction. Ellipsoids are drawn at the 50% probability level with hydrogen atoms omitted.

https://doi.org/10.1021/jacs.4c10110
J. Am. Chem. Soc. 2024, 146, 28407−28413

nitrogen atoms of the cyclometalating ligand and the ancillary ligand is revealed. The most notable effect of the *N*-aryl substituents is on the dihedral angle between the six-member Pt-(Ar)acNac plane and the *N*-aryl ring (Figure S1). This angle increases from 62.66° for complex $\mathbf{1}^{\mathrm{H/Ph}}$ to 78.99° ($\mathbf{2}^{\mathrm{H/dmp}}$) and 84.21° ($\mathbf{6}^{\mathrm{CN/dipp}}$). These larger angles in complexes $\mathbf{2}^{\mathrm{H/dmp}}$ and $\mathbf{6}^{\mathrm{CN/dipp}}$ avoid unfavorable steric interactions between the phenyl ring of the C^N ligand and the *N*-aryl group of the ancillary ligand. Generally, the three crystallographically characterized structures have very similar metrics otherwise, with no notable changes in the bond lengths or angles.

Electrochemical Properties. Cyclic voltammograms, presented in Figure 2, inform on the relative frontier orbital

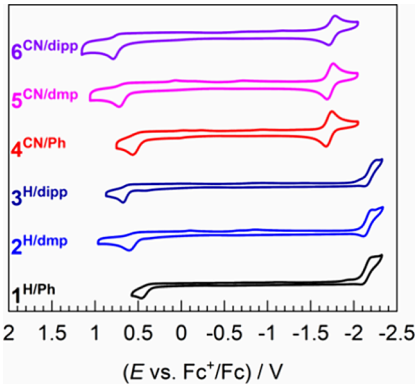

Figure 2. Cyclic voltammograms of complexes $\mathbf{1}^{\mathrm{H/Ph}}$–$\mathbf{6}^{\mathrm{CN/dipp}}$, recorded at 0.1 V/s in dichloromethane with 0.1 M $TBAPF_6$ as a supporting electrolyte. Potentials are referenced to an internal standard of ferrocene, and currents are normalized to bring all of the traces onto the same scale.

energies of the six complexes. The reduction potentials of complexes $\mathbf{1}^{\mathrm{H/Ph}}$–$\mathbf{3}^{\mathrm{H/dipp}}$ with C^N = piq occur near −2.2 V vs the ferrocenium/ferrocene (Fc^+/Fc) couple, and the potentials of complexes $\mathbf{4}^{\mathrm{CN/Ph}}$–$\mathbf{6}^{\mathrm{CN/dipp}}$ with C^N = piqCN are observed around −1.7 V. These features correspond to the reduction of the C^N ligand. As such, the electron-withdrawing cyano group in C^N = piq stabilizes the C^N-centered LUMO and shifts the reduction to more positive potentials. The observed reduction potentials are essentially independent of the identity of the ancillary ligand (Table 1). This indicates a minimal

Table 1. Summary of Cyclic Voltammetry Data for Complex $\mathbf{1}^{\mathrm{H/Ph}}$–$\mathbf{6}^{\mathrm{CN/dipp}}$

complex	E^{red} ($[Pt]^{0/-}$)/V	E^{ox} ($[Pt]^{+/0}$)/V[a]
$\mathbf{1}^{\mathrm{H/Ph}}$	−2.15	+0.46
$\mathbf{2}^{\mathrm{H/dmp}}$	−2.16	+0.61
$\mathbf{3}^{\mathrm{H/dipp}}$	−2.19	+0.68
$\mathbf{4}^{\mathrm{CN/Ph}}$	−1.72	+0.57
$\mathbf{5}^{\mathrm{CN/dmp}}$	−1.73	+0.72
$\mathbf{6}^{\mathrm{CN/dipp}}$	−1.75	+0.79

[a]Irreversible wave. $E_{p,a}$ is reported.

perturbation of the C^N-centered LUMO energies with the change of the ancillary ligands. The reduction waves are quasi-reversible in the C^N = piq complexes and fully reversible when C^N = piqCN. In all cases, peak-to-peak separations (ΔE_p) are ca. 60–80 mV, similar to other cyclometalated platinum complexes assigned to have quasi-reversible or reversible reduction waves,[13,43] and in the C^N = piqCN series near-unity current ratios ($i_{p,a}/i_{p,c}$) signify complete reversibility.

In contrast, the E^{ox} values, corresponding to the one-electron oxidation of the complexes, are strongly dependent on the identity of the ancillary ligand. In all cases, an irreversible oxidation wave was observed with a 0.1 V/s scan rate. Significant anodic shifts of ca. 0.2 V are observed with more sterically encumbered (Ar)acNac ligands, in both the piq and piqCN series. In both cases, by introducing methyl groups in ortho position, from (Ph)acNac to (dmp)(Ph)acNac, an anodic shift of 0.15 V was observed. A further increase in steric bulk by replacing the methyl groups with isopropyl groups results in a larger anodic shift of 0.22 V relative to (Ph)acNac. This shift runs counter to the expected electron-donating characteristics of alkyl groups, and its origin is not entirely clear. However, in square-planar platinum complexes the oxidation wave is often irreversible due to axial coordination upon accessing the formally Pt(III) state,[43,44] and the sterically blocking substituents in the (dmp)acNac and (dipp)acNac complexes may inhibit that process and render the complexes more difficult to oxidize. Consistent with this proposal, the crystal structures (Figure 1) of the bulkier (dmp)acNac and (dipp)acNac complexes ($\mathbf{2}^{\mathrm{H/dmp}}$ and $\mathbf{6}^{\mathrm{CN/dipp}}$) show the alkyl substituents protruding over the Pt center, in the region where the d_{z^2} orbital involved in the oxidation event and axial coordination resides.

Photophysical Properties. UV–vis absorption spectra of all complexes, recorded in toluene, are normalized and overlaid in Figures S2 and S3 and shown individually in Figures S4–S9. In the absorption spectra, intense bands from 300 to 400 nm are assigned to spin-allowed, ligand-centered (LC) $\pi \rightarrow \pi^*$ transitions of the cyclometalating ligands and ancillary ligands. Weaker absorption bands are assigned to metal-to-ligand charge transfer (MLCT) transitions, i.e., $5d(\mathrm{Pt}) \rightarrow \pi^*$-(C^N).[13,45,46] In complexes with C^N = piq this MLCT band occurs near 450 nm, and it shifts to near 500 nm in the C^N = piqCN series, consistent with the stabilization of the LUMO that is inferred from the cyclic voltammetry measurements described above. The (Ar)acNac substituents have minimal influences on the positions of the UV–vis absorption bands (Figures S2 and S3).

Room-temperature photoluminescence spectra of the six platinum(II) complexes are overlaid and displayed in Figure 3. A summary of the steady-state and time-resolved emission data, recorded in deoxygenated toluene, is presented in Table 2. The excitation spectra were also collected for all complexes and shown in Figures S4–S9. Well-overlapping absorption and excitation spectra were observed for all complexes, which indicate there are no impurities or aggregated states contributing to the observed luminescence. As shown in Figure 3, the photoluminescence of all complexes occurs in the red region with two vibronic peaks clearly resolved and a third observed as a shoulder. The λ_{0-0}, which is the shortest wavelength peak of the vibronic progression and represents radiative decay from the zeroth vibrational level of the triplet excited state to the zeroth vibrational level of the ground state, depends on the C^N ligand. In the piq complexes λ_{0-0} is observed around 600 nm and with the addition of the cyano group to the quinolyl ring in the piqCN complexes, the λ_{0-0} red shifts to around 630 nm. The PL maxima are nearly identical in each subset of three compounds with the same C^N ligand, showing no systematic dependence on the

https://doi.org/10.1021/jacs.4c10110
J. Am. Chem. Soc. 2024, 146, 28407–28413

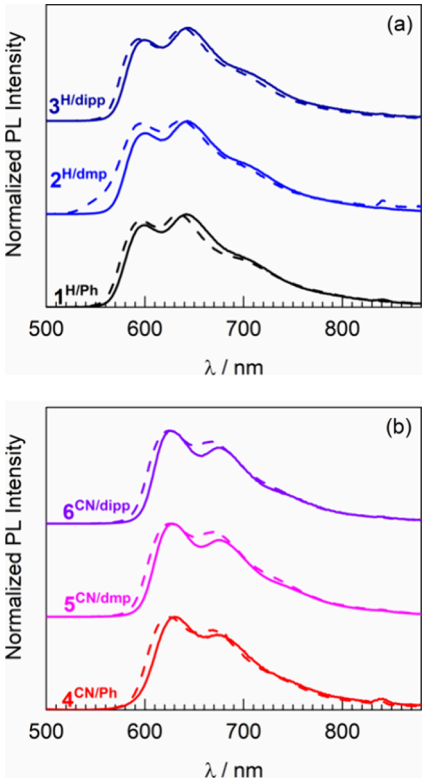

Figure 3. Stacked room temperature emission spectra of complexes with (a) C^N = piq ($\mathbf{1}^{\mathbf{H/Ph}}$–$\mathbf{3}^{\mathbf{H/dipp}}$), and (b) C^N = piqCN ($\mathbf{4}^{\mathbf{CN/Ph}}$–$\mathbf{6}^{\mathbf{CN/dipp}}$) in toluene (solid lines) and PMMA film (dashed line).

(Ar)acNac substituents. There is a slight difference in vibronic structure between piq complexes $\mathbf{1}^{\mathbf{H/Ph}}$–$\mathbf{3}^{\mathbf{H/dipp}}$ and piqCN complexes $\mathbf{4}^{\mathbf{CN/Ph}}$–$\mathbf{6}^{\mathbf{CN/dipp}}$. In the former, the λ_{0-1} peak is the maximum, whereas in the latter λ_{0-0} is the most intense. This change in vibronic structure suggests a more distorted, and likely more ligand-localized state in the piq complexes (i.e., a larger Huang–Rhys parameter),[47,48] versus a more delocalized emissive state when C^N = piqCN, with less excited-state structural distortion.

In each series of complexes, the (Ar)acNac steric profile has a profound impact on the excited-state dynamics. Comparing the all-oxygen donor ancillary ligand in Pt(piq)(acac) to its (Ph)acNac congener $\mathbf{1}^{\mathbf{H/Ph}}$, we observed a decrease in k_r value that led to a ca. 4-fold decrease in Φ_{PL}. This stands in contrast to previously reported Ir(piq)$_2$(L^X) complexes, where the same substitution results in a ca. 4-fold *increase* in k_r and one of the highest phosphorescence quantum yields observed in the red region (Φ_{PL} = 0.80). Undeterred, we recognized that steric modifications in (Ar)acNac ligands are accessible in square-planar complexes and hypothesized they could have substantial impacts on the excited-state dynamics. Augmenting the steric profile from (Ph)acNac ($\mathbf{1}^{\mathbf{H/Ph}}$) to (dmp)acNac ($\mathbf{2}^{\mathbf{H/dmp}}$) essentially reversed the downturn, with an increase in k_r and a decrease in k_{nr} resulting in an increase in quantum yield from 0.061 (complex $\mathbf{1}^{\mathbf{H/Ph}}$) to 0.24 (complex $\mathbf{2}^{\mathbf{H/dmp}}$). However, with even more sterically encumbering substituents on the ancillary ligand, k_{nr} increases, as seen in complex $\mathbf{3}^{\mathbf{H/dipp}}$ with (dipp)acNac, and Φ_{PL} decreases.

In the C^N = piqCN series ($\mathbf{4}^{\mathbf{CN/Ph}}$–$\mathbf{6}^{\mathbf{CN/dipp}}$), the effects of the (Ar)acNac ligand are broadly similar, but even more beneficial to the observed photoluminescence quantum yields. The k_r values are significantly higher with the cyano-substituted cyclometalating ligand; in the piq series k_r maximized at 0.70 × 10^{-5} s^{-1} (acac), but in the piqCN series all k_r values are larger than that with a maximum k_r of 2.3 × 10^{-5} s^{-1} ($\mathbf{4}^{\mathbf{CN/Ph}}$). These larger k_r values support the idea that excited-state ^{3}MLCT character is enhanced with piqCN complexes.[35] In complexes $\mathbf{4}^{\mathbf{CN/Ph}}$–$\mathbf{6}^{\mathbf{CN/dipp}}$, sterically encumbering substituents on the (Ar)acNac have a large and beneficial effect on the nonradiative rate constant. Changing from (Ph)acNac ($\mathbf{4}^{\mathbf{CN/Ph}}$) to (dmp)acNac ($\mathbf{5}^{\mathbf{CN/dmp}}$), we observe a large increase in quantum yield from 0.030 to 0.51 due to a ca. 70-fold decrease in k_{nr}. Complex $\mathbf{6}^{\mathbf{CN/dipp}}$, with (dipp)acNac, has nearly identical decay kinetics and Φ_{PL} as complex $\mathbf{5}^{\mathbf{CN/dmp}}$. Both complexes $\mathbf{5}^{\mathbf{CN/dmp}}$ and $\mathbf{6}^{\mathbf{CN/dipp}}$ have Φ_{PL} more than 0.5, very good for the red region of the spectrum and particularly noteworthy in the context of bis-bidentate cyclometalated platinum complexes where photoluminescence quantum yields below 0.2 are often observed.[13,49−55]

The photoluminescence spectra were also recorded in PMMA (PMMA = poly(methyl methacrylate)) thin films at 2 wt % in platinum complex, with the data summarized in Figure 3 and Table 3. In most cases, the quantum yields are higher in PMMA films than in solution, mainly due to a decrease in k_{nr}, although for $\mathbf{5}^{\mathbf{CN/dmp}}$ and $\mathbf{6}^{\mathbf{CN/dipp}}$ photoluminescence quantum yields in solution and PMMA are nearly identical. Both unencumbered analogues $\mathbf{1}^{\mathbf{H/Ph}}$ and $\mathbf{4}^{\mathbf{CN/Ph}}$ (L^X = (Ph)acNac) have Φ_{PL} = 0.44 in PMMA film, sharp increases from 0.061 and 0.030 in solution, respectively. We find that in these complexes that lack steric bulk on the (Ar)acNac ligand, immobilization in the film has a much more pronounced effect on k_{nr}. In PMMA, the (Ar)acNac all have higher photoluminescence quantum yields than their acac analogues, by as much as 2-fold (C^N = piq) and 1.5-fold (C^N = piqCN). A small but significant increase in k_r contributes to the higher quantum yields in the (Ar)acNac

Table 2. Summary of Room-Temperature Photoluminescence Data for Complexes in Toluene

complex	λ_{em}/nm	Φ_{PL}	τ/μs	(k_r[a] × 10^{-5}/s^{-1})/(k_{nr}[a] × 10^{-5}/s^{-1})
piq-acac	597, 646	0.23	3.3	0.70/2.3
$\mathbf{1}^{\mathbf{H/Ph}}$	600, 642	0.061	2.1	0.29/4.4
$\mathbf{2}^{\mathbf{H/dmp}}$	601, 643	0.24	4.0	0.60/1.9
$\mathbf{3}^{\mathbf{H/dipp}}$	598, 644	0.16	2.5	0.62/3.4
piqCN-acac	630, 685	0.34	3.6	0.94/1.8
$\mathbf{4}^{\mathbf{CN/Ph}}$	630, 673	0.030	0.13	2.3/75
$\mathbf{5}^{\mathbf{CN/dmp}}$	628, 674	0.51	4.2	1.2/1.2
$\mathbf{6}^{\mathbf{CN/dipp}}$	626, 676	0.54	4.5	1.2/1.0

[a] $k_r = \Phi/\tau$ and $k_{nr} = (1 - \Phi)/\tau$.

https://doi.org/10.1021/jacs.4c10110
J. Am. Chem. Soc. 2024, 146, 28407−28413

Table 3. Summary of Room-Temperature Photoluminescence Data for Complexes in 2 wt % PMMA Film

complex	λ_{em}/nm	Φ_{PL}	$\tau/\mu s$	(k_r[a] × 10^{-5}/s^{-1})/(k_{nr}[a] × 10^{-5}/s^{-1})
piq-acac	595, 642	0.22	4.5	0.49/1.7
$\mathbf{1}^{H/Ph}$	597, 635	0.44	4.7	0.94/1.2
$\mathbf{2}^{H/dmp}$	596, 638	0.32	4.4	0.73/1.5
$\mathbf{3}^{H/dipp}$	594, 639	0.38	5.2	0.73/1.2
piqCN-acac	627, 678	0.39	4.5	0.87/1.4
$\mathbf{4}^{CN/Ph}$	624, 667	0.44	4.2	1.0/1.3
$\mathbf{5}^{CN/dmp}$	626, 669	0.58	4.7	1.2/0.89
$\mathbf{6}^{CN/dipp}$	626, 668	0.53	4.7	1.1/1.0

[a] $k_r = \Phi/\tau$ and $k_{nr} = (1 - \Phi)/\tau$.

series when measured in PMMA. As with the data in toluene solution (Table 2), for a given C^N ligand the quantum yield values measured in PMMA film increase when steric bulk is added to the (Ar)acNac ligand but do not differ much between the (dmp)acNac and (dipp)acNac analogues, with $\mathbf{3}^{H/dipp}$ having a slightly higher Φ_{PL} than $\mathbf{2}^{H/dmp}$, and $\mathbf{6}^{CN/dipp}$ having a slightly lower Φ_{PL} than $\mathbf{5}^{CN/dmp}$. Thus, while adding steric bulk to the (Ar)acNac ligand is beneficial, there does not seem to be a clear advantage of the bulkiest (dipp)acNac analogue over (dmp)acNac.

To determine whether the (Ar)acNac steric profile influences aggregation in condensed phases, further study was conducted with representative complexes $\mathbf{2}^{H/dmp}$ and $\mathbf{4}^{CN/Ph}$ in PMMA films at varying concentrations between 1 and 10 wt %. As shown in Figures S10 and S11, the photoluminescence spectra are nearly identical at all concentrations, indicating that luminescent oligomeric or excimeric states are not forming in this concentration range. As shown in Table S2, the Φ_{PL} values maximize at 2 wt % and start to fall off at higher loading, indicating aggregation-caused quenching (ACQ).[56] Interestingly, the drop in Φ_{PL} is less pronounced in complex $\mathbf{2}^{H/dmp}$, which has the bulkier (dmp)acNac ligand, compared to complex $\mathbf{4}^{CN/Ph}$ which has the unsubstituted (Ph)acNac ligand. This outcome suggests that the sterically encumbering substituents play a role in inhibiting ACQ, in addition to their pronounced effects on excited-state dynamics.

CONCLUSIONS

In this work, we studied the effect of electron-rich and sterically encumbered β-ketominate ((Ar)acNac) ancillary ligands on the photophysical properties of cyclometalated platinum complexes. Most significantly, steric effects on the (Ar)acNac ancillary ligands play a dominant role in determining the excited-state dynamics and optimizing photoluminescence quantum yields. Whereas solution quantum yields in the unsubstituted (Ph)acNac complexes are substantially lower than the reference acac compounds, addition of alkyl substituents to the *N*-aryl rings brings about substantial increases. Of the two cyclometalating ligands studied, cyano-substituted piqCN results in deeper red phosphorescence and higher quantum yields, particularly in $\mathbf{5}^{CN/dmp}$ and $\mathbf{6}^{CN/dipp}$, which feature the encumbered (Ar)-acNac ancillary ligands and have photoluminescence quantum yields exceeding 0.5 in solution and PMMA films. The piqCN complexes ($\mathbf{4}^{CN/Ph}$–$\mathbf{6}^{CN/dipp}$) have larger k_r values, which in combination with qualitative analysis of their vibronic structure indicates enhanced MLCT character in the excited states compared to piq complexes ($\mathbf{1}^{H/Ph}$–$\mathbf{3}^{H/dipp}$). This work shows that judicious steric tuning of electron-rich ancillary ligands and substituents on the cyclometalating ligand can be combined as a viable strategy to obtain high photoluminescence quantum yields in the red region, which represents a significant challenge in bis-bidentate cyclometalated platinum complexes.

ASSOCIATED CONTENT

Supporting Information

The Supporting Information is available free of charge at https://pubs.acs.org/doi/10.1021/jacs.4c10110.

Experimental details, X-ray crystallographic summary table, UV–vis absorption and excitation spectra, photoluminescence spectra at varying concentration, and NMR spectra (PDF)

Accession Codes

CCDC 2370944–2370946 contain the supplementary crystallographic data for this paper. These data can be obtained free of charge via www.ccdc.cam.ac.uk/data_request/cif, or by emailing data_request@ccdc.cam.ac.uk, or by contacting The Cambridge Crystallographic Data Centre, 12 Union Road, Cambridge CB2 1EZ, UK; fax: + 44 1223 336033.

AUTHOR INFORMATION

Corresponding Author

Thomas S. Teets − *Department of Chemistry, University of Houston, Houston, Texas 77204, United States;* orcid.org/0000-0002-7471-8467; Email: tteets@central.uh.edu

Author

Sungwon Yoon − *Department of Chemistry, University of Houston, Houston, Texas 77204, United States*

Complete contact information is available at: https://pubs.acs.org/10.1021/jacs.4c10110

Notes

The authors declare no competing financial interest.

ACKNOWLEDGMENTS

The authors acknowledge the National Science Foundation (grant numbers CHE-1846831 and CHE-2348784) for funding this research.

REFERENCES

(1) Costa, R. D.; Ortí, E.; Bolink, H. J.; Monti, F.; Accorsi, G.; Armaroli, N. Luminescent Ionic Transition-Metal Complexes for Light-Emitting Electrochemical Cells. *Angew. Chem., Int. Ed.* **2012**, *51* (33), 8178–8211.

(2) Chuang, W.-T.; Chen, B.-S.; Chen, K.-Y.; Hsieh, C.-C.; Chou, P.-T. Fluorescent Protein Red Kaede Chromophore; One-Step, High-Yield Synthesis and Potential Application for Solar Cells. *Chem. Commun.* **2009**, *45*, 6982−6984.
(3) Schmid, L.; Glaser, F.; Schaer, R.; Wenger, O. S. High Triplet Energy Iridium(III) Isocyanoborato Complex for Photochemical Upconversion, Photoredox and Energy Transfer Catalysis. *J. Am. Chem. Soc.* **2022**, *144* (2), 963−976.
(4) Zuo, Z.; Ahneman, D. T.; Chu, L.; Terrett, J. A.; Doyle, A. G.; MacMillan, D. W. C. Merging Photoredox with Nickel Catalysis: Coupling of α-Carboxyl Sp3-Carbons with Aryl Halides. *Science* **2014**, *345* (6195), 437−440.
(5) Yoon, T. P.; Ischay, M. A.; Du, J. Visible Light Photocatalysis as a Greener Approach to Photochemical Synthesis. *Nat. Chem.* **2010**, *2* (7), 527−532.
(6) Maillard, J.; Rumble, C. A.; Fürstenberg, A. Red-Emitting Fluorophores as Local Water-Sensing Probes. *J. Phys. Chem. B* **2021**, *125* (34), 9727−9737.
(7) Shimomura, N.; Egawa, Y.; Miki, R.; Fujihara, T.; Ishimaru, Y.; Seki, T. A Red Fluorophore Comprising a Borinate-Containing Xanthene Analogue as a Polyol Sensor. *Org. Biomol. Chem.* **2016**, *14* (42), 10031−10036.
(8) Chan, M. H.-Y.; Leung, S. Y.-L.; Yam, V. W.-W. Rational Design of Multi-Stimuli-Responsive Scaffolds: Synthesis of Luminescent Oligo(Ethynylpyridine)-Containing Alkynylplatinum(II) Polypyridine Foldamers Stabilized by Pt···Pt Interactions. *J. Am. Chem. Soc.* **2019**, *141* (31), 12312−12321.
(9) Baldo, M. A.; O'Brien, D. F.; You, Y.; Shoustikov, A.; Sibley, S.; Thompson, M. E.; Forrest, S. R. Highly Efficient Phosphorescent Emission from Organic Electroluminescent Devices. *Nature* **1998**, *395*, 151−154.
(10) Lee, J.; Chen, H.-F.; Batagoda, T.; Coburn, C.; Djurovich, P. I.; Thompson, M. E.; Forrest, S. R. Deep Blue Phosphorescent Organic Light-Emitting Diodes with Very High Brightness and Efficiency. *Nat. Mater.* **2016**, *15* (1), 92−98.
(11) Chen, Z.; Wang, L.; Su, S.; Zheng, X.; Zhu, N.; Ho, C.-L.; Chen, S.; Wong, W.-Y. Cyclometalated Iridium(III) Carbene Phosphors for Highly Efficient Blue Organic Light-Emitting Diodes. *ACS Appl. Mater. Interfaces* **2017**, *9* (46), 40497−40502.
(12) Sarma, M.; Tsai, W.-L.; Lee, W.-K.; Chi, Y.; Wu, C.-C.; Liu, S.-H.; Chou, P.-T.; Wong, K.-T. Anomalously Long-Lasting Blue PhOLED Featuring Phenyl-Pyrimidine Cyclometalated Iridium Emitter. *Chem.* **2017**, *3* (3), 461−476.
(13) Brooks, J.; Babayan, Y.; Lamansky, S.; Djurovich, P. I.; Tsyba, I.; Bau, R.; Thompson, M. E. Synthesis and Characterization of Phosphorescent Cyclometalated Platinum Complexes. *Inorg. Chem.* **2002**, *41* (12), 3055−3066.
(14) Kourkoulos, D.; Karakus, C.; Hertel, D.; Alle, R.; Schmeding, S.; Hummel, J.; Risch, N.; Holder, E.; Meerholz, K. Photophysical Properties and OLED Performance of Light-Emitting Platinum(II) Complexes. *Dalton Trans.* **2013**, *42* (37), 13612−13621.
(15) Bullock, J. D.; Salehi, A.; Zeman, C. J.; Abboud, K. A.; So, F.; Schanze, K. S. In Search of Deeper Blues: *Trans*-N-Heterocyclic Carbene Platinum Phenylacetylide as a Dopant for Phosphorescent OLEDs. *ACS Appl. Mater. Interfaces* **2017**, *9* (47), 41111−41114.
(16) Hang, X.-C.; Fleetham, T.; Turner, E.; Brooks, J.; Li, J. Highly Efficient Blue-Emitting Cyclometalated Platinum(II) Complexes by Judicious Molecular Design. *Angew. Chem., Int. Ed.* **2013**, *52* (26), 6753−6756.
(17) Jiang, Z.; Wang, J.; Gao, T.; Ma, J.; Liu, Z.; Chen, R. Rational Design of Axially Chiral Platinabinaphthalenes with Aggregation-Induced Emission for Red Circularly Polarized Phosphorescent Organic Light-Emitting Diodes. *ACS Appl. Mater. Interfaces* **2020**, *12* (8), 9520−9527.
(18) Shafikov, M. Z.; Daniels, R.; Pander, P.; Dias, F. B.; Williams, J. A. G.; Kozhevnikov, V. N. Dinuclear Design of a Pt(II) Complex Affording Highly Efficient Red Emission: Photophysical Properties and Application in Solution-Processible OLEDs. *ACS Appl. Mater. Interfaces* **2019**, *11* (8), 8182−8193.
(19) Roy, S.; Lopez, A. A.; Yarnell, J. E.; Castellano, F. N. Metal−Metal-to-Ligand Charge Transfer in Pt(II) Dimers Bridged by Pyridyl and Quinoline Thiols. *Inorg. Chem.* **2022**, *61* (1), 121−130.
(20) Tuong Ly, K.; Chen-Cheng, R.-W.; Lin, H.-W.; Shiau, Y.-J.; Liu, S.-H.; Chou, P.-T.; Tsao, C.-S.; Huang, Y.-C.; Chi, Y. Near-Infrared Organic Light-Emitting Diodes with Very High External Quantum Efficiency and Radiance. *Nat. Photonics* **2017**, *11* (1), 63−68.
(21) Borek, C.; Hanson, K.; Djurovich, P. I.; Thompson, M. E.; Aznavour, K.; Bau, R.; Sun, Y.; Forrest, S. R.; Brooks, J.; Michalski, L.; Brown, J. Highly Efficient, Near-Infrared Electrophosphorescence from a Pt−Metalloporphyrin Complex. *Angew. Chem., Int. Ed.* **2007**, *46* (7), 1109−1112.
(22) Xiong, W.; Meng, F.; You, C.; Wang, P.; Yu, J.; Wu, X.; Pei, Y.; Zhu, W.; Wang, Y.; Su, S. Molecular Isomeric Engineering of Naphthyl-Quinoline-Containing Dinuclear Platinum Complexes to Tune Emission from Deep Red to near Infrared. *J. Mater. Chem. C* **2019**, *7* (3), 630−638.
(23) Wang, L.; Miao, J.; Zhang, Y.; Wu, C.; Huang, H.; Wang, X.; Yang, C. Discrete Mononuclear Platinum(II) Complexes Realize High-Performance Red Phosphorescent OLEDs with EQEs of up to 31.8% and Superb Device Stability. *Adv. Mater.* **2023**, *35* (32), No. 2303066.
(24) Zhang, Y.; Yin, Z.; Meng, F.; Yu, J.; You, C.; Yang, S.; Tan, H.; Zhu, W.; Su, S. Tetradentate Pt(II) 3,6-Substitued Salophen Complexes: Synthesis and Tuning Emission from Deep-Red to near Infrared by Appending Donor-Acceptor Framework. *Org. Electron.* **2017**, *50*, 317−324.
(25) Zhang, Y.; Meng, F.; You, C.; Yang, S.; Xiong, W.; Wang, Y.; Su, S.; Zhu, W. Achieving NIR Emission for Tetradentate Platinum (II) Salophen Complexes by Attaching Dual Donor-Accepter Frameworks in the Heads of Salophen. *Dyes Pigments* **2017**, *138*, 100−106.
(26) Wu, W.; Guo, H.; Wu, W.; Ji, S.; Zhao, J. Long-Lived Room Temperature Deep-Red/Near-IR Emissive Intraligand Triplet Excited State (^{3}IL) of Naphthalimide in Cyclometalated Platinum(II) Complexes and Its Application in Upconversion. *Inorg. Chem.* **2011**, *50* (22), 11446−11460.
(27) Mandapati, P.; Braun, J. D.; Lozada, I. B.; Williams, J. A. G.; Herbert, D. E. Deep-Red Luminescence from Platinum(II) Complexes of *N*^*N*^−^*N*-Amido Ligands with Benzannulated *N*-Heterocyclic Donor Arms. *Inorg. Chem.* **2020**, *59* (17), 12504−12517.
(28) Kim, J.-M.; Cheong, K.; Jiang, J.; Jeon, S. O.; Hong, W. P.; Lee, J. Y. Tetradentate Pt Complexes for Organic Light-Emitting Diodes. *Trends Chem.* **2023**, *5* (4), 267−278.
(29) Allison, I.; Lim, H.; Shukla, A.; Ahmad, V.; Hasan, M.; Deshmukh, K.; Wawrzinek, R.; McGregor, S. K. M.; Clegg, J. K.; Divya, V. V.; Govind, C.; Suresh, C. H.; Karunakaran, V.; Narayanan Unni, K. N.; Ajayaghosh, A.; Namdas, E. B.; Lo, S.-C. Solution Processable Deep-Red Phosphorescent Pt(II) Complex: Direct Conversion from Its Pt(IV) Species via a Base-Promoted Reduction. *ACS Appl. Electron. Mater.* **2019**, *1* (7), 1304−1313.
(30) Chan, A. K.-W.; Ng, M.; Wong, Y.-C.; Chan, M.-Y.; Wong, W.-T.; Yam, V. W.-W. Synthesis and Characterization of Luminescent Cyclometalated Platinum(II) Complexes with Tunable Emissive Colors and Studies of Their Application in Organic Memories and Organic Light-Emitting Devices. *J. Am. Chem. Soc.* **2017**, *139* (31), 10750−10761.
(31) Englman, R.; Jortner, J. The Energy Gap Law for Radiationless Transitions in Large Molecules. *Mol. Phys.* **1970**, *18*, 145.
(32) Caspar, J. V.; Meyer, T. J. Application of the Energy Gap Law to Nonradiative. *Excited-State Decay. J. Phys. Chem.* **1983**, *87* (6), 952−957.
(33) Yersin, H.; Finkenzeller, W. J. Triplet Emitters for Organic Light-Emitting Diodes: Basic Properties. In *Highly Efficient OLEDs with Phosphorescent Materials*; John Wiley & Sons, Ltd, 2007; 1−97.
(34) Yersin, H. Triplet Emitters for Organic Light - Emitting Diodes: Basic Properties. In *Highly efficient OLEDs with phosphorescent materials*; Yersin, H., Ed.; WILEY-VCH: Weinheim, 2008; 1−97.

https://doi.org/10.1021/jacs.4c10110
J. Am. Chem. Soc. 2024, 146, 28407−28413

(35) Yersin, H.; Rausch, A. F.; Czerwieniec, R.; Hofbeck, T.; Fischer, T. The Triplet State of Organo-Transition Metal Compounds. Triplet Harvesting and Singlet Harvesting for Efficient OLEDs. *Coord. Chem. Rev.* **2011**, *255* (21), 2622−2652.
(36) Lai, P.-N.; Brysacz, C. H.; Alam, M. K.; Ayoub, N. A.; Gray, T. G.; Bao, J.; Teets, T. S. Highly Efficient Red-Emitting Bis-Cyclometalated Iridium Complexes. *J. Am. Chem. Soc.* **2018**, *140* (32), 10198−10207.
(37) Yoon, S.; Teets, T. S. Red to Near-Infrared Phosphorescent Ir(III) Complexes with Electron-Rich Chelating Ligands. *Chem. Commun.* **2021**, *57* (16), 1975−1988.
(38) Kabir, E.; Wu, Y.; Sittel, S.; Nguyen, B.-L.; Teets, T. S. Improved Deep-Red Phosphorescence in Cyclometalated Iridium Complexes *via* Ancillary Ligand Modification. *Inorg. Chem. Front.* **2020**, *7* (6), 1362−1373.
(39) Yoon, S.; Teets, T. S. Enhanced Deep Red to Near-Infrared (DR-NIR) Phosphorescence in Cyclometalated Iridium(III) Complexes. *Inorg. Chem. Front.* **2022**, *9* (24), 6544−6553.
(40) Tsuboyama, A.; Iwawaki, H.; Furugori, M.; Mukaide, T.; Kamatani, J.; Igawa, S.; Moriyama, T.; Miura, S.; Takiguchi, T.; Okada, S.; Hoshino, M.; Ueno, K. Homoleptic Cyclometalated Iridium Complexes with Highly Efficient Red Phosphorescence and Application to Organic Light-Emitting Diode. *J. Am. Chem. Soc.* **2003**, *125* (42), 12971−12979.
(41) Chen, Z.; Zhang, H.; Wen, D.; Wu, W.; Zeng, Q.; Chen, S.; Wong, W.-Y. A Simple and Efficient Approach toward Deep-Red to near-Infrared-Emitting Iridium(Iii) Complexes for Organic Light-Emitting Diodes with External Quantum Efficiencies of over 10%. *Chem. Sci.* **2020**, *11* (9), 2342−2349.
(42) Choung, K. S.; Islam, M. D.; Guo, R. W.; Teets, T. S. Monometallic and Bimetallic Platinum Complexes with Fluorinated β-Diketiminate Ligands. *Inorg. Chem.* **2017**, *56* (22), 14326−14334.
(43) Kvam, P.-I.; Puzyk, M. V.; Balashev, K. P.; Songstad, J.; Lundberg, C.; Arnarp, J.; Björk, L.; Gawinecki, R. Spectroscopic and Electrochemical Properties of Some Mixed-Ligand Cyclometalated Platinum(II) Complexes Derived from 2-Phenylpyridine. *Acta Chem. Scand.* **1995**, *49*, 335−343.
(44) Davies, J. A.; Uma, V. A Re-Investigation of the Electrochemistry of Isomeric $[PtCl_2(PR_3)_2]$ Complexes by Cyclic Voltammetry. *Inorg. Chim. Acta* **1983**, *76*, L305−L307.
(45) Lanoë, P.-H.; Moreno-Betancourt, A.; Wilson, L.; Philouze, C.; Monnereau, C.; Jamet, H.; Jouvenot, D.; Loiseau, F. Neutral Heteroleptic Cyclometallated Platinum(II) Complexes Featuring 2-Phenylbenzimidazole Ligand as Bright Emitters in Solid State and in Solution. *Dyes Pigments* **2019**, *162*, 967−977.
(46) Chassot, L.; Mueller, E.; Von Zelewsky, A. Cis-Bis(2-Phenylpyridine)Platinum(II) (CBPPP): A Simple Molecular Platinum Compound. *Inorg. Chem.* **1984**, *23* (25), 4249−4253.
(47) Huang, K.; Rhys, A. Theory of Light Absorption and Non-Radiative Transitions in *F*-Centres. *Proc. R. Soc. Lond. Ser. Math. Phys. Sci.* **1950**, *204* (1078), 406−423.
(48) Lo, S.-C.; Shipley, C. P.; Bera, R. N.; Harding, R. E.; Cowley, A. R.; Burn, P. L.; Samuel, I. D. W. Blue Phosphorescence from Iridium(III) Complexes at Room Temperature. *Chem. Mater.* **2006**, *18* (21), 5119−5129.
(49) Chan, J. C.-H.; Lam, W. H.; Wong, H.-L.; Zhu, N.; Wong, W.-T.; Yam, V. W.-W. Diarylethene-Containing Cyclometalated Platinum(II) Complexes: Tunable Photochromism via Metal Coordination and Rational Ligand Design. *J. Am. Chem. Soc.* **2011**, *133* (32), 12690−12705.
(50) Rajendra Kumar, G.; Thilagar, P. Tuning the Phosphorescence and Solid State Luminescence of Triarylborane-Functionalized Acetylacetonato Platinum Complexes. *Inorg. Chem.* **2016**, *55* (23), 12220−12229.
(51) Hruzd, M.; Kahlal, S.; Le Poul, N.; Wojcik, L.; Cordier, M.; Saillard, J.-Y.; Rodríguez-López, J.; Robin-le Guen, F.; Gauthier, S.; Achelle, S. Phosphorescent Cyclometalated Platinum(II) Complexes with Phenyldiazine N^C Ligands. *Dalton Trans.* **2023**, *52* (7), 1927−1938.
(52) Shavaleev, N. M.; Adams, H.; Best, J.; Edge, R.; Navaratnam, S.; Weinstein, J. A. Deep-Red Luminescence and Efficient Singlet Oxygen Generation by Cyclometalated Platinum(II) Complexes with 8-Hydroxyquinolines and Quinoline-8-Thiol. *Inorg. Chem.* **2006**, *45* (23), 9410−9415.
(53) Zhang, H.; Liu, C.; Du, C.; Zhang, B. Efficiently Red Emitting Cycloplatinated(II) Complexes Supported by N^O and N^P Benzimidazole Ancillary Ligands. *J. Organomet. Chem.* **2022**, *960*, No. 122237.
(54) Qiao, L.; Luan, X.; Low, K.-H.; Zhou, Y.; Zhang, Y.; Che, C.-M. Cyclometalated Pt(II)C^N Phosphors Bearing a Bis-(Diphenylphorothioyl) Amide Ligand: Synthesis and Photophysical Properties. *J. Coord. Chem.* **2024**, *77* (9−10), 1042−1057.
(55) Montagu, J.; Gontard, G.; Williams, J. A. G.; Moussa, J. Cyclometallated Platinum(II) Complexes Featuring an Unusual, C^N-Coordinating Pyridyl-Pyridylidene Ligand and L X Coligands: Synthesis, Structures and Dual Luminescence Behavior. *Eur. J. Inorg. Chem.* **2023**, *26* (32), No. e202300487.
(56) Wu, Y.; Wen, Z.; Wu, J. I.-C.; Teets, T. S. Efficient Deep Blue Platinum Acetylide Phosphors with Acyclic Diaminocarbene Ligands. *Chem.−Eur. J.* **2020**, *26* (68), 16028−16035.

https://doi.org/10.1021/jacs.4c10110
J. Am. Chem. Soc. 2024, 146, 28407−28413